Signatures of diffusion and ballistic transport in the stiffness, dynamical correlation functions, and statistics of one-dimensional systems

Subroto Mukerjee[1,2] and B. Sriram Shastry[3]
[1]*Department of Physics, University of California, Berkeley, California 94720, USA*
[2]*Materials Sciences Division, Lawrence Berkeley National Laboratory, Berkeley, California 94720, USA*
[3]*Department of Physics, University of California, Santa Cruz, California 95064, USA*
(Received 27 February 2008; revised manuscript received 30 April 2008; published 24 June 2008)

Integrable and nonintegrable systems have very different transport properties. In this paper, we highlight these differences for specific one-dimensional models of interacting lattice fermions. The technique used is a finite temperature numerical calculation of the adiabatic stiffness (also called the Drude weight or charge stiffness) and isothermal stiffness (also called the "Meissner" stiffness) in electrical and energy transport, and the momentum dependent dynamical conductivities $\sigma(q,\omega)$ and $\kappa(q,\omega)$. We apply a flux twist to break the Kramers degeneracy; thus, allowing us to focus on the effect of the dynamical degeneracies in the integrable system. In this situation, we show that the isothermal stiffness goes to zero rapidly with the system size for both types of systems even at high temperatures; while the adiabatic stiffness appears to go to zero in the nonintegrable system and to a finite value in the integrable one. We analyze this difference in terms of the statistics of the current matrix elements and the degeneracies of the systems, and show that in the integrable system, despite the presence of degeneracies, the dominant contribution to the adiabatic stiffness comes from large-current-carrying nondegenerate states. We also show that energy transport at nonzero ω and q occurs within a banded continuum in the integrable system indicative of ballistic transport while the nonintegrable system shows diffusion but with the existence of overdamped excitations at large values of momentum.

DOI: 10.1103/PhysRevB.77.245131 PACS number(s): 72.10.Bg, 72.15.−v

I. INTRODUCTION AND ISSUES IN TRANSPORT IN ONE-DIMENSIONAL SYSTEMS

The study of the nature of transport in one-dimensional (1D) systems at finite and zero temperatures has been an area of long-standing interest.[1–7] These systems are different from their higher dimensional counterparts in several ways. For instance, a low-temperature effective theory of 1D interacting fermions can be formulated in terms of free bosonic oscillators ("the Luttinger liquid"), which shows that they are significantly different from the Fermi liquids that are encountered in higher dimensions.[1] Another interesting feature of 1D systems is the possibility of them being integrable, where there is an infinite family of nontrivial mutually commuting operators that also commute with the Hamiltonian. A classic example is the 1D Hubbard model, which possesses an infinite number of dynamical operators, which are analogous in spirit to the Runge–Lenz vector for the hydrogen atom.[8] Since these operators correspond to the symmetries of the system, physical processes are strongly influenced by the constraints, thus, imposed. In particular, transport and scattering processes are expected to be considerably modified in the presence of such symmetries.[9]

Several integrable systems such as the 1D Hubbard model and the XXZ spin chain are also exactly solvable using the Bethe Ansatz.[10,11] While this technique has proven to be successful for calculating many static properties, it has not been very useful in the calculation of transport coefficients. Moreover, exact solutions have been difficult to apply to calculations at high temperature. Thus, while the static behavior of integrable systems is fairly well understood at low temperatures, several questions remain about the nature of transport in these systems, especially at high temperature. In the absence of any reliable analytical techniques, most studies take recourse to numerics. In this context, exact diagonalization on finite-sized systems has proven to be a particularly useful technique, since one can obtain all the energy eigenvalues and eigenstates required for high temperature calculations.[2–6,12–14] The fact that the systems are one dimensional implies that one can approximate the thermodynamic limit even for systems of modest sizes.[15,16]

A study of transport requires the identification of current operators. For a given Hamiltonian H, the current operators can be obtained from the density operators with which they satisfy continuity equations. In one dimension, the charge and energy current operators [$J^e(k)$ and $J^E(k)$, respectively] at a momentum k are given by

$$J^e(k) = \frac{1}{k}[n(-k),H], \quad J^E(k) = \frac{1}{k}[h(-k),H], \tag{1}$$

where $n(k)$ and $h(k)$ are the charge and energy densities at momentum k, respectively. In the rest of the paper, the $k=0$ values of the charge and energy current operators will be denoted by J^e and J^E, respectively.

In calculating electrical transport in linear response, the central formula of interest is the Kubo formula,

$$\sigma(\omega) = \frac{\pi}{\hbar}\bar{D}_e\delta(\omega) + \frac{\pi}{L}\left(\frac{1-e^{-\beta\omega}}{\omega}\right)\sum_{\epsilon_n\neq\epsilon_m}|J^e_{nm}|^2\delta(\epsilon_n-\epsilon_m-\hbar\omega). \tag{2}$$

Here, σ is the conductivity, ω the frequency, and L the size of the 1D system. J^e_{nm} is the electrical current matrix element between the eigenstates n and m of the system of energy, ϵ_n and ϵ_m. $p_n=\exp(-\epsilon_n/k_BT)$ is the Boltzmann weight

of the state n. $\bar{D}_e$ is the adiabatic charge stiffness (or simply the charge stiffness), which is also called the Drude weight. It is thus named because Eq. (2) is derived by studying the adiabatic evolution of an equilibrium state disturbed in the infinitely remote past by the application of a time-dependent perturbation. Similar Kubo formulae can be written down for the thermal and Peltier conductivities $\kappa(\omega)$, and $\alpha(\omega)$, which involve the heat current for the former, and the heat and electrical currents for the latter. The form of Eq. (2) shows that the first term contributes to transport only at exactly zero frequency while the second, to transport only at nonzero frequencies. Thus, the zero frequency electrical conductivity of a system will formally be infinite if $\bar{D}_e$ is nonzero. The expression for $\bar{D}_e$, also obtainable from linear response theory, is[17]

$$\bar{D}_e = \frac{1}{L}\left[\langle\tau\rangle - \hbar \sum_{\epsilon_n \neq \epsilon_n} \frac{p_n - p_m}{\epsilon_m - \epsilon_n} |J^e_{nm}|^2\right]. \tag{3}$$

Here, $\langle \ldots \rangle$ denotes thermal averaging and the operator τ is given by,

$$\tau = -\lim_{k\to 0} \frac{1}{k}[J^e(k), n(-k)]. \tag{4}$$

Similar to the case of the Kubo formula, an analogous formula can be derived for the Drude weights corresponding to the thermal and thermoelectric transports.

In terms of the quantities defined above, one can define yet another stiffness called the charge isothermal stiffness or the "Meissner stiffness" D_e,[17]

$$D_e = \frac{1}{L}\left[\langle\tau\rangle - \hbar \sum \frac{p_n - p_m}{\epsilon_m - \epsilon_n} |J^e_{nm}|^2\right]. \tag{5}$$

The analogous isothermal stiffnesses can be defined for thermal and thermoelectric transport. D_e arises in a study of the Byers–Yang type curvature of the free energy with respect to a flux through a ring.[18] The difference between Eqs. (3) and (5) is that the sum over the energies excludes equal energies in the former but not in the latter. Thus,

$$\bar{D}_e - D_e = \frac{\hbar}{k_B T L} \sum_{\epsilon_n = \epsilon_m} p_n |J^e_{nm}|^2. \tag{6}$$

If D_e is known to be zero, the Drude weight is given by the left-hand side of Eq. (6) and is the expression that has been quite extensively used for this quantity in the literature. However, it is not always true that D_e is zero, as in the case of a superconductor. In this case, the calculation of the Drude weight requires the use of Eq. (3). In this paper, we will show, with specific examples, that the isothermal stiffness is zero for both integrable and nonintegrable 1D systems at finite temperature.

We now describe the qualitative features of the transport in different systems in terms of these stiffnesses. A perfect metal is distinguished from a superconductor by the absence of the Meissner effect, although both share an infinite conductivity at zero temperature. This absence of dissipation in the static limit is in contrast to the behavior of normal (dirty) metallic systems and corresponds to $Re\sigma(\omega) \propto \delta(\omega)$. As temperature is increased, the superconductor continues to have an infinite conductivity and displays the Meissner effect for as long as it is still in the ordered phase. On the other hand, very generally, one would expect a perfect metal to become resistive at finite temperature owing to inelastic scattering processes. This is indeed what happens in a nonintegrable system, which we will call a nonintegrable metal (NIM). In one dimension, however, another fundamental kind of metallic system is possible, corresponding to an integrable system, which we will call an integrable metal (IM). Such a system can display characteristics that are different from both an NIM and a superconductor, such as an infinite conductivity *at all temperatures* and no Meissner effect. This exemption from inelastic scattering of the IM as opposed to the NIM is attributed to the constraints imposed by the conservation laws and is directly tracked in this paper by calculating various transport stiffnesses. In terms of the transport stiffnesses described above, one would expect a superconductor to have nonzero values of both D_e and $\bar{D}_e$ at finite temperature. Since there are no superconductors (no long range order) at finite temperature in 1D, these quantities will be zero in the thermodynamic limit. However, for a finite-sized system, they can be finite. Both D_e and $\bar{D}_e$ should be zero for an NIM. For an IM, D_e is expected to be zero at all temperatures but not necessarily $\bar{D}_e$. While a nonzero D_e implies a nonzero $\bar{D}_e$, the converse is not true. As can be seen from Eqs. (3) and (5), the distinction between D_e and $\bar{D}_e$ resides in the relative statistical weight of states with equal energy, and raises the question of the relative weight of this manifold of equal energy states and how this varies between an NIM and IM.

The quantity $\bar{D}_e$ has been numerically calculated at finite temperature in different 1D models. The most popular of these is the XXZ spin chain, which can be mapped onto a model of spinless fermions with nearest-neighbor hopping and interaction, and the Hubbard model. The XXZ model is the one we study here in terms of spinless fermions and focus on the Heisenberg point. The Drude weight of this model at finite temperature has been studied by various techniques in the past, and results have been obtained to support both claims that it is zero[7,19] and finite.[4,6]

$\bar{D}_e$ is given by the left-hand side of Eq. (6) if D_e is zero, as is true (and will be numerically demonstrated for specific models in this paper) for the IM and NIM at finite temperature. If the system is time-reversal invariant, the only contribution to $\bar{D}_e$ comes from states that are degenerate and related to each other by time reversal. Nondegenerate states do not carry any current. In an interesting study, it was argued that the finite Drude weight of the IM in a time-reversal invariant situation is due to a finite fraction of degenerate states related by time reversal.[4] Each state in such a pair of degenerate states has a different (discrete) value of total momentum. However, this study did not address the issue of the contribution of the degenerate states due to dynamical symmetries to the Drude weight. The current operator (and the Hamiltonian) commutes with the total momentum and, thus, for a fixed number of particles, the contribution to $\bar{D}_e$ is the sum of the contributions from the different sectors of total momentum. Thus, an interesting question one can ask is *how*

do states that are degenerate with other states at the same value of momentum contribute to the Drude weight? Unlike in a nonintegrable system, these degeneracies would be present in integrable systems and their existence is a direct consequence of the presence of dynamical conservation laws. This issue is complementary to that addressed in Ref. 4.

Transport at finite frequencies in both integrable and nonintegrable systems is also of great interest. The nature of the excitations of these systems is often reflected in the frequency ω and momentum q dependent transport coefficients. For instance, in the simple example of noninteracting particles, a banded continuum in the values of the ω and q dependent electrical and thermal conductivities, $\sigma(q,\omega)$ and $\kappa(q,\omega)$ is obtained.[20] This continuum is related to the fact that the charge and heat current operators in this simple system commute with the Hamiltonian and transport is ballistic. The Drude weight in this simple model is finite at all temperatures with $\sigma(q=0,\omega)$ and $\kappa(q=0,\omega)\propto\delta(\omega)$, a consequence of the fact that the respective operators commute with the Hamiltonian. An interesting question is, how much of this behavior survives in the presence of interactions and what role does integrability play, if at all? In an NIM, signatures of diffusion have been seen at high temperatures and a hydrodynamic theory of transport predicts a nonanalytic form for $\sigma(q=0,\omega)$ at small values of ω.[2]

We have been motivated by the issues mentioned above to undertake an exhaustive study of a typical IM and NIM in this paper by computing their exact energy spectra and all the current matrix elements, and, consequently, the transport stiffnesses and dynamic conductivities. This exercise is done in 1D with a popular model, the $t-t'-V$ model of spinless electrons, where a single parameter t' corresponding to second neighbor hops destroys the integrability but lets the system remain a perfect metal (a NIM). $t'=0$ produces an IM. In contrast to electrons with spin, we are able to go to somewhat bigger system sizes, which is necessary to extract meaningful results for the stiffnesses. Indeed, all stiffnesses are nonzero for finite systems and it is only the systematics of their size dependence that gives us reliable information on the large size behavior. Since we are interested in the contribution of only the dynamical degeneracies, we apply an irrational flux twist to lift the Kramer's degeneracy. Every state now potentially carries a current and we determine which of these have partner degenerate states due to a dynamical symmetry and how they contribute to the Drude weight. We find that after the Kramer's degeneracy has been lifted in the integrable system, the dominant contribution to the Drude weight appears to be from large-current-carrying nondegenerate states. We also study the complete dynamic conductivity $\sigma(q,\omega)$ and thermal conductivity $\kappa(q,\omega)$ using these matrix elements after using an appropriate scheme for binning the discrete data points to obtain continuous functions. This gives us detailed information on the fluctuations of electrical and energy currents and densities, and also of the nature of the excitations in the many-body spectra. We find that the integrable system displays the banded behavior like in noninteracting systems for $\kappa(q,\omega)$ and to a lesser extent in $\sigma(q,\omega)$. The nonintegrable system, on the other hand, shows evidence of diffusive behavior with the presence of overdamped oscillations at high values of momentum.[21,22]

II. THE MODEL

The $t-t'-V$ model of spinless fermions on a 1D ring is given by the Hamiltonian,

$$H=-t\sum_j (c_{j+1}^\dagger c_j + c_j^\dagger c_{j+1}) - t'\sum_j (c_{j+2}^\dagger c_j + c_j^\dagger c_{j+2}) + V\sum_j n_j n_{j+1}. \quad (7)$$

For concreteness, we choose the value of t and V to be 1.0 and 2.0, respectively. With $t'=0$, this model can be mapped onto the integrable spin-1/2 Heisenberg ring using a Jordan–Wigner transformation. We set $t'=1$ when we model the NIM. Chains of length 6–18 are studied, and we focus on half-filling for definiteness. The Hamiltonian Eq. (7) is then exactly numerically diagonalized. We would like to emphasize that our conclusions vis-à-vis integrability and nonintegrability are quite general and independent of the microscopic parameters and the filling. We also apply an irrational flux twist to break time-reversal invariance in studying the stiffnesses in both the IM and the NIM. This also gets rid of an odd-even particle number effect in the IM and does not affect the integrability. The local number density, used to calculate the currents in Eq. (1), is the number of carriers at every site and the energy density is defined, such that the hopping energy is shared equally among the sites participating in the hopping process, as is the interaction energy (the "midpoint convention"). We have checked to see that other local definitions do not alter the results. D_α and $\bar{D}_\alpha$ for electrical and energy transport are numerically calculated at different temperatures ($T=1/\beta$ is measured in units of t).[23,24]

III. STIFFNESSES OF THE INTEGRABLE AND NONINTEGRABLE MODELS

Here, we show only the results for electrical transport in Fig. 1 but the ones for the energy transport display exactly the same qualitative behavior. Our results, up to the largest system size ($L=18$), seem to indicate that the charge stiffness of the IM is nonzero, as one would expect from considerations of ballistic transport.[25] A confirmation of this, to rule out any slow decay with L, is currently beyond the range of accessible system sizes through exact diagonalization. However, recent results on larger systems using quantum Monte Carlo (QMC) simulations also appear to find a finite charge stiffness.[26] The NIM, on the other hand, appears to show a clear (exponential with power-law corrections) decay of $\bar{D}_e$ with the system size. This behavior persists to temperatures higher than the typical energy scales in the problem and, *in fact, even up to infinite temperature*. These results are interesting since they show that the system is aware of its integrability or nonintegrability (which are quantum concepts), even up to infinite temperature where one might expect classical physics to apply. D_e rapidly vanishes in the thermodynamic limit in both systems (even without the flux twist). This shows in particular that the IM, despite having an infinite conductivity at $\omega=0$, is not a superconductor. It is a curious fact that D_e is positive at small system sizes in the

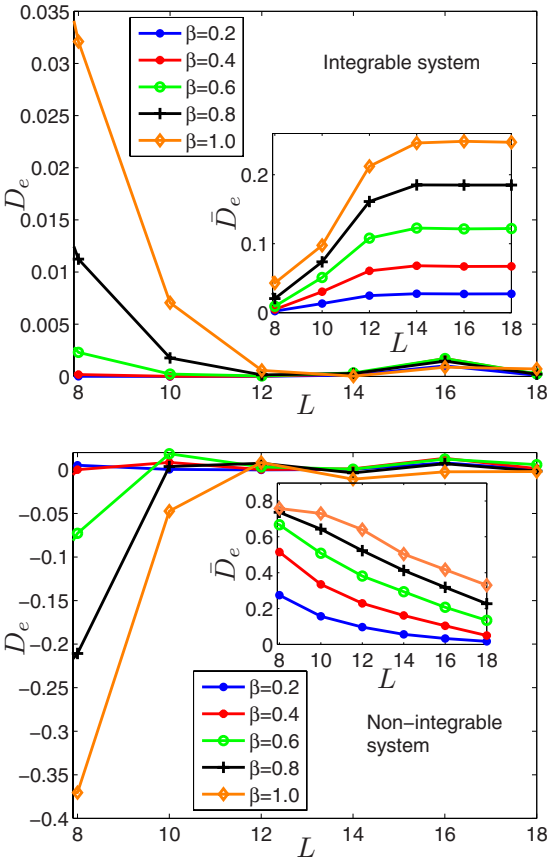

FIG. 1. (Color online) (Top) The isothermal and the adiabatic (inset) stiffnesses for electrical transport in the integrable system at various values of β with an irrational flux twist. It can be seen that the former tends to zero rapidly with increasing system size while the latter appears to go to a constant, indicative of ballistic transport. (Bottom) The same stiffnesses for electrical transport in the nonintegrable system again with an irrational flux twist for consistency. Both tend to zero with the system size but D_e does so more rapidly.

IM and negative in the NIM. The situation is reversed without a flux twist.

We now outline a comparative statistical study of $\bar{D}_e$ in the two systems to investigate the role of dynamical degeneracies. While D_e in both systems rapidly decreases to zero with the system size, $\bar{D}_e$ appears to decrease (more slowly than D_e) to zero in the NIM but goes to a constant in the IM. Thus, at this level of analysis, it appears that $\bar{D}_e$ goes to a constant for the IM and decreases (presumably to zero) for the NIM up to the largest system size ($L=18$) studied. At $L=18$, there is however not a significant difference in magnitude between $\bar{D}_e$ in both systems. This is essentially because of the fact that the microscopic parameters of the two systems are different and $\bar{D}_e$ is a quantity with the dimensions of energy over length whose magnitude would have a dependence on the microscopic parameters of the model. To enable a better comparison of $\bar{D}_E$ in the IM and the NIM at a given L, we first place them on equal footing by dividing it by $\langle\Phi\rangle$ and removing the inherent scale dependence on the microscopic parameters. For the largest system sizes ($L=18$), we find that this scale-independent $\bar{D}_e$ is about 8–15 times larger in the IM than the NIM for the values of β considered; thus, indicating that $\bar{D}_e$ for the IM is indeed larger in magnitude than the NIM, as one would expect from the considerations of the introduction. However, we emphasize that a comparison of the behavior in the thermodynamic limit of the two systems is only meaningful by examining the size dependence of $\bar{D}_e$ and not just the values at one size.

Since D_e is zero at large L, $\bar{D}_e$ is given by Eq. (6). The scale-independent $\bar{D}_e$ in the IM can be written as

$$\bar{D}_e = \bar{D}_e^d + \bar{D}_e^{nd}. \tag{8}$$

$$\bar{D}_e^{nd} = \frac{\hbar}{k_B T L} \sum_n{}' p_n |J_{nn}^e|^2, \tag{9}$$

where Σ_n' indicates a summation over states which have *no degeneracies* within a given momentum sector. $\bar{D}_e^d$ then represents the contribution from states, which are members of degenerate multiplets within a momentum sector. By parsing $\bar{D}_e$ this way, we can directly focus on the relative contribution of states with degeneracies and those without by computing the ratio $\bar{D}_e^d/\bar{D}_e^{nd}$.

Let us first consider the NIM. For a fixed number of particles and in the presence of an irrational flux twist, the only conservation law is that of total momentum. Thus, there are no degeneracies in any of the momentum sectors except perhaps for accidental degeneracies, which do not scale with the system size. Therefore, in this case, the only contribution to $\bar{D}_e$ comes from $\bar{D}_e^{nd}$.

The IM is more interesting. The dynamical symmetries ensure that there are degeneracies within each momentum sector, and both $\bar{D}_e$ and $\bar{D}_e^{nd}$ are nonzero. One can now ask the following question: Is the large scale-independent $\bar{D}_e$ in the IM, compared to the NIM, due to a large contribution from $\bar{D}_e^d$ (degeneracies) or $\bar{D}_e^{nd}$ (nondegenerate states) or both? To answer this question, we have studied the statistics of the number of degeneracies and the current matrix elements (and, hence, $\bar{D}_e^d$ and $\bar{D}_e^{nd}$) in the two systems. We find that at $L=16$ in the IM, about 10% of the states are pairwise degenerate with a very negligible fraction of higher order degeneracies. Furthermore, most of the degeneracies occur among the states with total lattice momentum 0 or π. Quantitatively, about 75% of the states in each of the $q=0$ and π sectors are degenerate with a very negligible fraction in any of the other sectors. The total number of states in each momentum sector is about the same. We find that in this system, the ratio $\bar{D}_e^d/\bar{D}_e^{nd}$ is at most 0.2 for the values of β investigated. On the other hand, the ratio of $\bar{D}_e^{nd}$ between the IM and NIM is about 8–15. Thus, we come to the following interesting conclusion: Even though the IM has degeneracies, their contribution to the charge stiffness is not significant. *The larger scale-independent* $\bar{D}_e$ in the IM, compared to the NIM, is primarily a consequence of the nondegenerate states carrying larger currents. A further observation that is

being investigated in more detail is that the eigenvalues of the current operator in a given degenerate subsector in the IM are always approximately equal to each other.

We emphasize that the aim of this study is not to merely determine whether or not the Drude weight of the model we are studying is finite but to analyze the effect of the dynamical conservation laws on this quantity. To that end, we have determined the contribution to the (finite) Drude weight of the integrable system of the states with and without degeneracies due to the dynamical symmetries and shown that the dominant contribution comes from large-current-carrying nondegenerate states. It is interesting that the QMC study, previously mentioned also finds that the Drude weight of a nonintegrable model (obtained by introducing second nearest neighbor hopping) at finite temperature is finite, in contradiction to previous studies.[26] Exact diagonalization studies of the model in Ref. 26 have been performed for systems up to size $L=24$, on the basis of which it was concluded that the Drude weight at finite temperature is zero in this system.[3] The nonintegrable model we study here using exact diagonalization also appears to have a rapidly decreasing Drude weight with increasing system size. Our model has an integrability breaking next-nearest-neighbor hopping term while the one studied in Ref. 26 has a next-nearest-neighbor interaction term. The difference vis-à-vis the finiteness of the Drude weight in the two systems might have something to do with this fact. Whether this is indeed the case and the contradiction between the QMC and exact diagonalization studies is specific to only certain types of models requires further investigation beyond the focus of this paper.

IV. TRANSPORT AT FINITE q AND ω

Having demonstrated the difference between integrability and nonintegrability in zero frequency transport, we now focus on transport at finite frequency (ω) and momentum (q). The q and ω dependent conductivities are given by,

$$A_\alpha(q,\omega) = c(\omega) \sum_{p,\epsilon_n \neq \epsilon_m} p_n |\langle n|J_\alpha(q)|m\rangle|^2 \delta(\epsilon_m - \epsilon_n - \hbar\omega), \tag{10}$$

where $c(\omega)=\frac{\pi}{L}(\frac{1-e^{-\beta\omega}}{\omega})$, $A_e(q,\omega)=\sigma(q,\omega)$, and $A_E(q,\omega)=\kappa(q,\omega)$. These conductivities can also be related to density–density correlation functions of the charge and energy.[5] We choose a small value of $\beta=0.001$, since numerical exact diagonalization for a calculation of this sort is most efficient only at very high temperatures.[2] The irrational flux twist turns out to be unimportant to the results here. $\sigma(q,\omega)$ and $\kappa(q,\omega)$, as functions of ω (in units of the hopping t) for different values of q (going from 0 to 8) for an $L=16$ IM, are shown in Fig. 2. $\kappa(q=0,\omega)\propto\delta(\omega)$, since $[J_E(q=0),H]=0$ but $[J_e(q=0),H]\neq 0$ and, thus, $\sigma(q=0,\omega)$ has some structure at $\omega\neq 0$. A more interesting feature is that $\kappa(q,\omega)$ is nonzero only within a band of frequencies for small values of q and goes to zero abruptly at the boundaries of the band. Moreover, this band shifts to higher frequencies with increasing q. The dispersion of these banded modes appears to be roughly linear (at small q), which is consistent with considerations of ballistic transport. For instance, the situation is similar to the case of free fermions where a ballistic transport causes a similar banded structure in $\kappa(q,\omega)$. The common feature of this IM and free fermions is integrability, which it appears is strongly associated with the concept of ballistic transport. $\sigma(q,\omega)$ does not prominently display the same banded feature as $\kappa(q,\omega)$, presumably due to the fact that $[J_e(q=0),H]\neq 0$, where the analogy with free fermions does not apply. Figure 3 shows the contour plots of $\sigma(q,\omega)$ and $\kappa(q,\omega)$ to better illustrate the banded nature of $\kappa(q,\omega)$ and enable comparison to $\sigma(q,\omega)$.

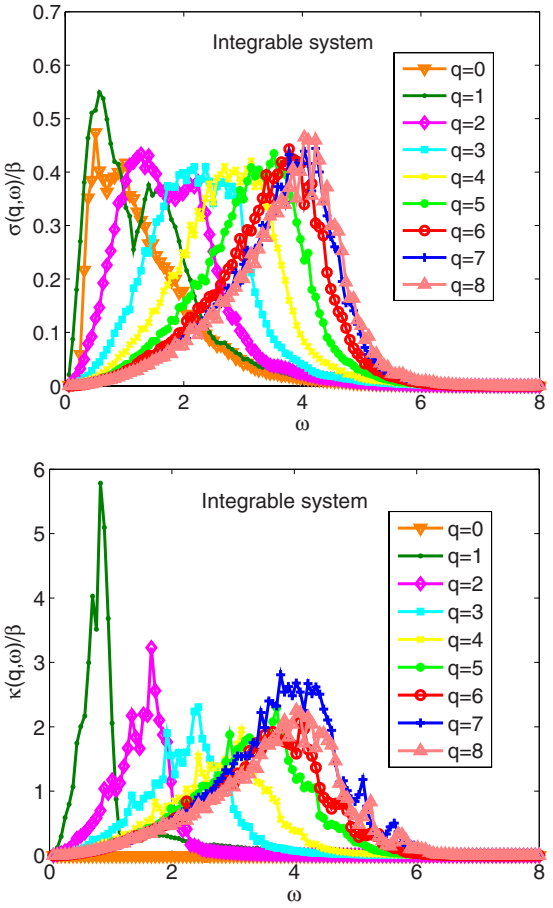

FIG. 2. (Color online) Plots of (above) $\sigma(q,\omega)$ and (below) $\kappa(q,\omega)$ vs ω for the integrable system with $L=16$ at $\beta=0.001$. It can be seen in the plot of $\kappa(q,\omega)$ that there is a band of frequencies for a given value of q, in which the value of $\kappa(q,\omega)$ is large and then abruptly falls to zero at the boundaries. This behavior is much less pronounced in $\sigma(q,\omega)$.

To compare and contrast the ballistic behavior of the IM to the NIM, we also present the numerical data for $\sigma(q,\omega)$ and $\kappa(q,\omega)$ for the latter. The plots of these quantities are shown in Fig. 4. Here, $[J_E(q=0),H]\neq 0$ and $\kappa(q=0,\omega)$ is nonzero at $\omega\neq 0$. Both $\sigma(q=0,\omega)$ and $\kappa(q=0,\omega)$ display a finite nonanalytic singularity at $\omega=0$, which has been attributed to diffusion and nonlinear hydrodynamics for the former.[2] In this system, $\kappa(q,\omega)$ does not display the banded behavior of the IM and gradually goes to zero with increasing ω for all q. This is indicative of diffusion in this system, which we have verified by also directly computing the density–density correlators. The features (bumps) at large

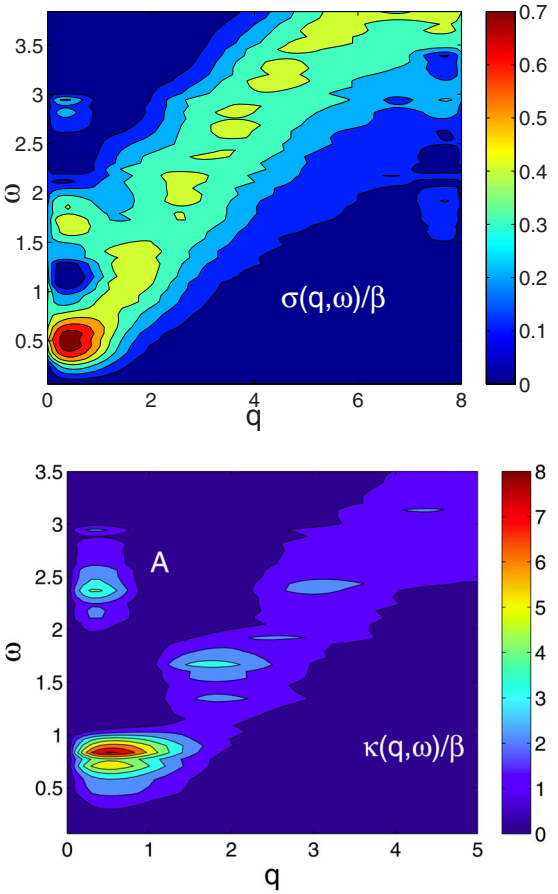

FIG. 3. (Color online) Colored contour plots of (above) $\sigma(q,\omega)$ and (below) $\kappa(q,\omega)$ for the IM with $L=16$ at $\beta=0.001$. The momentum $q=0$ to 8. An eighth order polynomial interpolation has been used to convert the discrete numerical data into a function of a continuous momentum variable q and the feature marked A on the lower plot is an artifact of that. The plot of $\kappa(q,\omega)$ shows the banded continuum in the center bounded by dark blue regions.

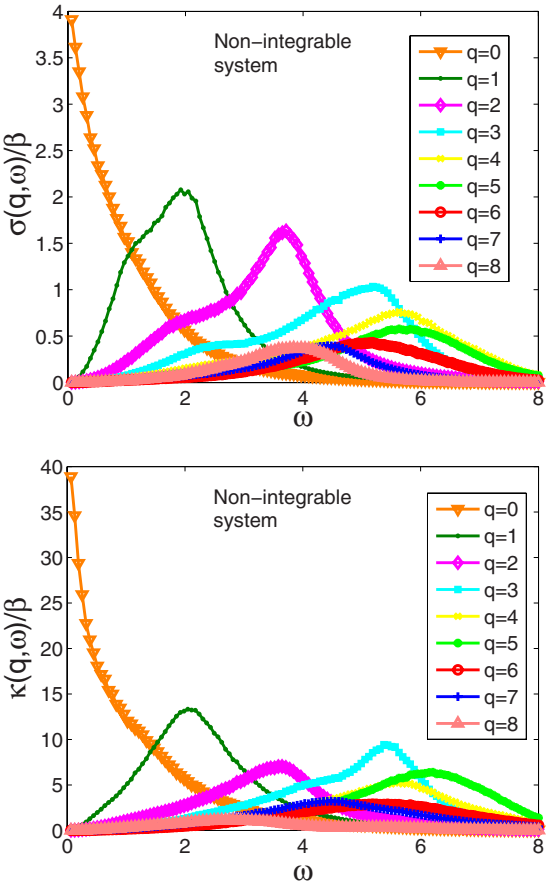

FIG. 4. (Color online) Plots of (above) $\sigma(q,\omega)$ and (below) $\kappa(q,\omega)$ vs ω for the NIM with $L=16$ at $\beta=0.001$. $\kappa(q,\omega)$ no longer displays the banded behavior of the integrable system and falls off gradually (and not abruptly) at higher frequencies. The peaks in both $\sigma(q,\omega)$ and $\kappa(q,\omega)$ at large q are also present in the density–density correlation functions, indicating the presence of overdamped excitations.

values of q and ω also appear in these correlators, indicating the presence of interesting overdamped excitations, which will be investigated in detail elsewhere.

To conclude, we have demonstrated that the IM shows several signs of ballistic behavior, as opposed to diffusion in the NIM. This is manifested in the adiabatic stiffnesses of the two systems. A statistical analysis of this quantity reveals that the contribution of degenerate states to the IM is not significant. The disappearance of the isothermal stiffness shows that the IM is not a superconductor. $\sigma(q,\omega)$ and $\kappa(q,\omega)$ in the IM and NIM are also consistent with ballistic transport and diffusion, respectively, with the former having a banded $\kappa(q,\omega)$ and the latter having overdamped excitations at large q.

ACKNOWLEDGMENTS

The authors wish to acknowledge conversations with J. O. Haerter, D. A. Huse, J. E. Moore, M. R. Peterson, and V. Oganeysan. S.M. thanks DOE for support and the IBM SUR program. B.S.S. acknowledges support from the DOE and the NSF.

[1] F. D. M. Haldane, J. Phys. C **14**, 2585 (1981).
[2] S. Mukerjee, V. Oganesyan, and D. A. Huse, Phys. Rev. B **73**, 035113 (2006).
[3] X. Zotos and P. Prelovsek, Phys. Rev. B **53**, 983 (1996).
[4] B. N. Narozhny, A. J. Millis, and N. Andrei, Phys. Rev. B **58**, R2921 (1998).
[5] F. Naef and X. Zotos, J. Phys.: Condens. Matter **10**, L183 (1998).
[6] F. Heidrich-Meisner, A. Honecker, D. C. Cabra, and W. Brenig, Phys. Rev. B **66**, 140406(R) (2002).
[7] X. Zotos, Phys. Rev. Lett. **82**, 1764 (1999).
[8] B. S. Shastry, Phys. Rev. Lett. **56**, 2453 (1986).

[9] X. Zotos, J. Phys. Soc. Jpn. **74**, 173 (2005).
[10] E. H. Lieb and F. Y. Wu, Phys. Rev. Lett. **20**, 1445 (1968).
[11] M. Takahashi and M. Suzuki, Prog. Theor. Phys. **48**, 2187 (1972).
[12] D. A. Rabson, B. N. Narozhny, and A. J. Millis, Phys. Rev. B **69**, 054403 (2004).
[13] K. Kudo and T. Deguchi, J. Phys. Soc. Jpn. **74**, 1992 (2005).
[14] F. Heidrich-Meisner, A. Honecker, D. C. Cabra, and P. W. Brenig, Physica B (Amsterdam) **359-361**, 1394 (2005).
[15] S. Fujimoto and N. Kawakami, Phys. Rev. Lett. **90**, 197202 (2003).
[16] J. V. Alvarez and C. Gros, Phys. Rev. Lett. **88**, 077203 (2002).
[17] B. S. Shastry, Phys. Rev. B **73**, 085117 (2006).
[18] T. Giamarchi and B. S. Shastry, Phys. Rev. B **51**, 10915 (1995).
[19] J. Benz, T. Fukui, A. Klumper, and C. Scheeren, J. Phys. Soc. Jpn. **74**, 181 (2005).
[20] T. Niemeijer, Physica (Amsterdam) **36**, 377 (1967).
[21] C. A. Stafford, A. J. Millis, and B. S. Shastry, Phys. Rev. B **43**, 13660 (1991).
[22] X. Zotos, F. Naef, and P. Prelovsek, Phys. Rev. B **55**, 11029 (1997).
[23] S. Kirchner, H. G. Evertz, and W. Hanke, Phys. Rev. B **59**, 1825 (1999).
[24] A. Rosch and N. Andrei, Phys. Rev. Lett. **85**, 1092 (2000).
[25] P. Jung, R. W. Helmes, and A. Rosch, Phys. Rev. Lett. **96**, 067202 (2006).
[26] D. Heidarian and S. Sorella, Phys. Rev. B **75**, 241104(R) (2007).